Vol. 663: 77–97, 2021
https://doi.org/10.3354/meps13647

MARINE ECOLOGY PROGRESS SERIES
Mar Ecol Prog Ser

Published March 31

High growth resilience of subarctic rhodoliths (*Lithothamnion glaciale*) to ocean warming and chronic low irradiance

David Bélanger[1,*], Patrick Gagnon[2]

[1]Department of Biology, Memorial University of Newfoundland, St. John's, NL A1B 3X9, Canada
[2]Department of Ocean Sciences, Ocean Sciences Centre, Memorial University of Newfoundland, St. John's, NL A1C 5S7, Canada

ABSTRACT: We paired a 361 d laboratory mesocosm experiment and a 383 d field experiment with rhodoliths (*Lithothamnion glaciale*) collected in Newfoundland (Canada) to test the overall hypothesis that growth in subarctic rhodoliths is chiefly controlled by irradiance. Rhodoliths in the laboratory were exposed to 1 of 5 seawater temperatures (ambient, 2, 4, 7, and 10°C) and 1 of 3 irradiances (low [0.02], intermediate [0.11], and high [0.27 mol photons m^{-2} d^{-1}]). Rhodoliths in the field were held in cages at 3 depths (8, 15, and 25 m). Laboratory results demonstrated that growth is unaffected by temperatures between ~1 and 16°C. Field results suggested that growth ceases at temperatures near or below 0.5°C and showed that the annual growth profile of *L. glaciale* comprises 3 distinct phases, namely 2 of positive growth separated by 1 of arrested growth, and that the switch from one phase to the next coincides with seasonal shifts in sea temperature and light regimes. Rhodoliths at 25 m appeared to utilize light nearly twice as efficiently as rhodoliths at 15 m, which enabled similar growth at both depths despite the ~60% lower irradiance at 25 m. We conclude that growth is chiefly controlled by irradiance and that temperature effects may override, but not interact with, those of irradiance during the coldest months of the year. Subarctic *L. glaciale* rhodoliths are resilient to changes in sea temperature over a relatively broad thermal range, with sustained growth even at temperatures above those normally observed during most of the year in Newfoundland coastal waters and northwards.

KEY WORDS: Coralline algae · Maerl · Temperature · Irradiance · Light · Mesocosm experiment · Seasonal variation · Mixed-effects models · Newfoundland

1. INTRODUCTION

Sea temperature is an important driver of metabolic and physiological responses in marine algae, with most species growing and reproducing within specific temperature ranges that often correlate with latitude (Lüning 1984). Temperature also varies with depth, more so in temperate seas where strong thermoclines can form during the warm season (Hickman et al. 2012) that place a higher demand on species as they approach their tolerance limits (Gillooly et al. 2001, Eggert 2012). By powering photosynthesis, solar radiation (irradiance), which attenuates as it penetrates the ocean (Wozniak & Dera 2007), also influences algal physiology and bathymetric distribution. Algae in the 3 major taxonomic groups (Chlorophyta, Ocrophyta, and Rhodophyta) have evolved photosynthetic characteristics to harvest light within specific depth ranges or parts of the light spectrum (Dring 1990, Figueroa et al. 1997), with some capacity to adapt to daily and seasonally changing light quality and quantity (Hanelt 1998, Figueroa et al. 2009).

Effects of changes in sea temperature and irradiance on algal growth are difficult to separate because

*Corresponding author: david.belanger@mun.ca

these 2 factors often co-vary and interact in the marine environment (White et al. 1997), while thermal optima for growth can vary with irradiance, and vice versa (Spilling et al. 2015). Few studies have tried to separate individual and interactive effects of temperature and irradiance on the physiology of coralline red algae. Adey (1970) concluded that temperature and irradiance simultaneously control growth in several boreal–subarctic crustose corallines, while Comeau et al. (2014) suggested that only low irradiance significantly decreases net calcification in the tropical crustose coralline *Hydrolithon reinboldii*. Such mixed results highlight the need for additional studies to tease apart effects of temperature and irradiance on coralline algal growth.

Rhodoliths are non-geniculate, unattached, benthic coralline red algae with highly calcified tissues that grow only a few millimetres per year (Foster 2001). Depending on species and environmental conditions, rhodoliths vary in size, shape, and growth form, ranging from small twig-like thalli to large (>10 cm across) and highly branched ellipsoids (Woelkerling et al. 1993). They thrive in all oceans from the low intertidal zone down to the lower photic zone, accumulating in structurally complex and biologically diverse communities known as rhodolith beds (Foster 2001). Despite the global distribution of rhodolith beds, their ecological importance as nursery habitats, and significant role in marine carbon cycling (van der Heijden & Kamenos 2015, Teed et al. 2020), only a handful of studies have examined the effects of changes in sea temperature and irradiance on rhodolith growth (Freiwald & Henrich 1994, Kamenos & Law 2010, Teichert & Freiwald 2014). For example, Blake & Maggs (2003) combined laboratory and field experiments to test the effects of water temperature and depth (a proxy for light) on the growth of several European corallines and concluded that responses are species-specific. Burdett et al. (2012) proposed that rhodoliths can adapt to low-light environments by adjusting their light saturation point. Although informative, these studies are entirely correlational, short term, or lack the necessary methodological rigor and temporal resolution for proper testing and partitioning of the effects of both factors on rhodolith growth. The need to characterize and predict rhodolith growth responses to individual and combined effects of changes in temperature and irradiance has become even more important with ongoing global ocean warming (Levitus et al. 2012) and increasing turbidity of coastal waters as a result of alteration to global hydrological cycles (Ahn et al. 2005, Ogston & Field 2010, Fabricius et al. 2013).

Given the slow growth of rhodoliths, long-term laboratory and field experiments are crucial to draw reliable conclusions about their growth response to environmental changes (Bélanger & Gagnon 2020). In the Northwest Atlantic, the coralline red alga *Lithothamnion glaciale* dominates coralline assemblages at depths of 15–25 m (Adey & Hayek 2011). *L. glaciale* rhodoliths and extensive rhodolith beds develop within this depth range along the coast of Newfoundland and Labrador, Canada (Gagnon et al. 2012, Adey et al. 2015, Millar & Gagnon 2018, Bélanger & Gagnon 2020, Teed et al. 2020). Rhodoliths in shallow (0–25 m deep) subtidal habitats of Newfoundland experience considerable seasonal variation in sea temperature (ca. −1 to 16°C) and irradiance (~0–14 mol photons m^{-2} d^{-1}; Caines & Gagnon 2012, Blain & Gagnon 2013, Gagnon et al. 2013, Frey & Gagnon 2015, Bélanger & Gagnon 2020, present study), and hence provide an excellent opportunity to improve our understanding of their resilience to variation in temperature and light availability.

In the present study, we paired a 361 d laboratory mesocosm experiment and a 383 d field experiment with Newfoundland *L. glaciale* to examine individual and interactive effects of water temperature and irradiance on rhodolith growth. Rhodoliths in the laboratory experiment experienced different combinations of controlled (from ~2 to 10°C) or naturally fluctuating (from ~1 to 16°C) water temperature and irradiance (from ~0.02 to 0.27 µmol m^{-2} d^{-1}). We predicted that growth would be unrelated to temperature, but would increase with irradiance. We held rhodoliths in the field experiment in cages at 3 depths (8, 15, and 25 m). We predicted that growth would decrease with increasing depth, and would vary seasonally with irradiance. These predictions stem from studies suggesting that growth in *L. glaciale* (and other *Lithothamnion* species) (1) does not correlate with seasonal changes in sea temperature (Kamenos & Law 2010, Darrenougue et al. 2013) and (2) correlates positively with intensity and duration of solar radiation (Teichert & Freiwald 2014).

2. MATERIALS AND METHODS

2.1. Rhodolith collection and staining

We carried out the 2 experiments described in Sections 2.2 and 2.3 with medium-sized (40–45 mm in diameter) *Lithothamnion glaciale* (Fig. 1A). Divers hand collected rhodoliths on 25 August 2012, at a depth of ~15 m, and bottom water temperature of

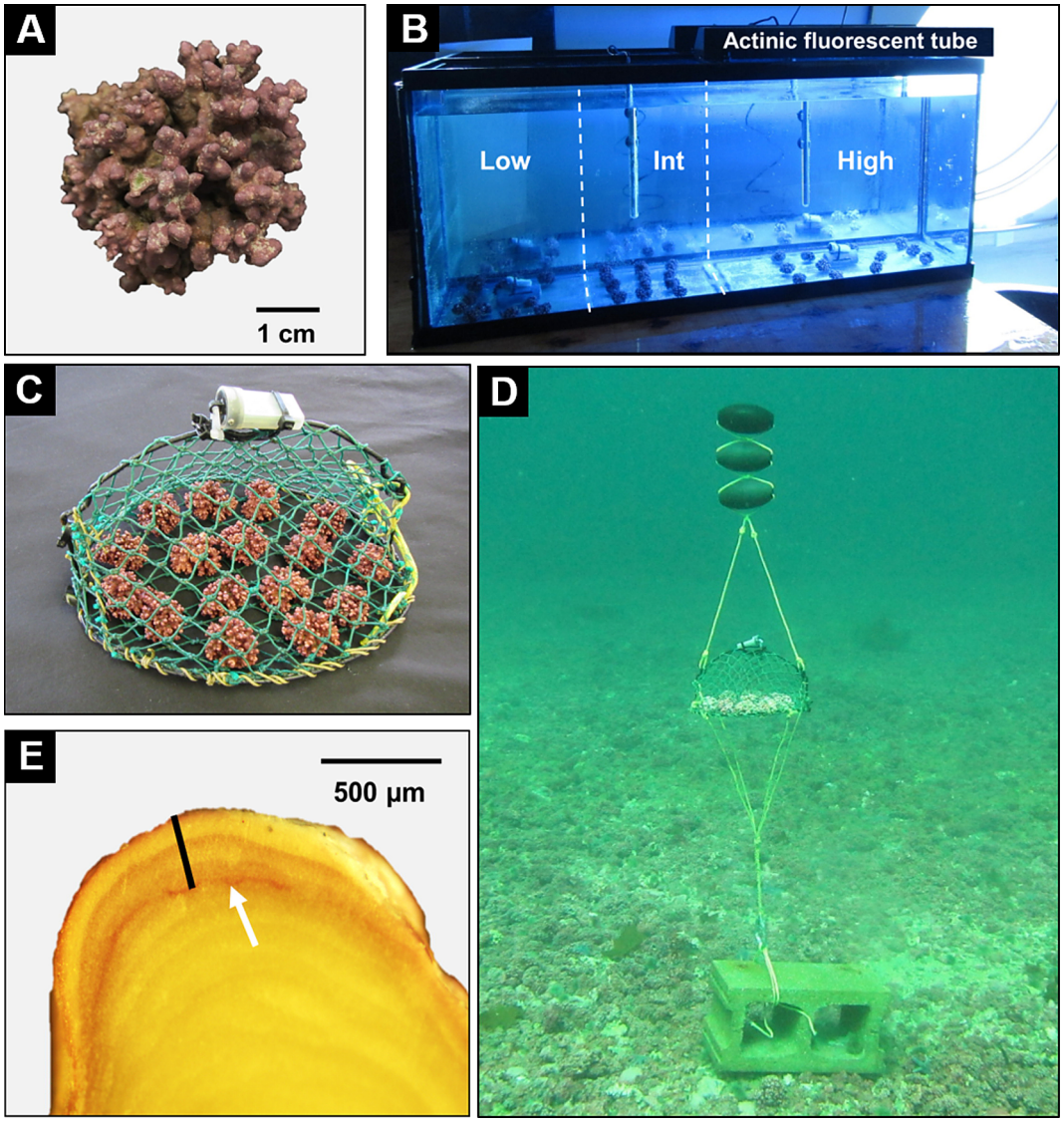

Fig. 1. (A) Shape (primarily spheroidal) and size of sample rhodolith used in laboratory mesocosm and field experiments. (B) One of the 5 mesocosms (180 l) with location of the 3 irradiance treatment sections (low, intermediate [Int], and high), 2 temperature loggers (bottom), actinic fluorescent tube, and circular window (right) overlooking Logy Bay, Newfoundland, Canada. (C) One of the rhodolith cages used in the field experiment (~25 cm diameter × 15 cm high) with a temperature and light logger attached to the top. (D) One of the cages attached to a concrete block and suspended in the water column by small floats at a depth of 15 m in the rhodolith bed in St. Philip's. (E) Longitudinal section of the tip of a rhodolith branch showing the stain mark (white arrow) used to measure growth, defined as the maximum length of the axis perpendicularly joining the stain mark and apex of the branch (black bar)

~13°C, in the middle of a relatively large (0.025 km^2) rhodolith bed off St. Philip's (47° 35′ 33″ N, 52° 53′ 33″ W) in Conception Bay, Newfoundland, Canada (see Gagnon et al. 2012 for a detailed description of the bed). Rhodoliths were transported in plastic containers filled with seawater to the Ocean Sciences Centre (OSC) of Memorial University of Newfoundland. Upon arrival at the OSC, we transferred rhodoliths into 2 glass tanks (180 l each, with a single layer of ~150 ind. $tank^{-1}$), each supplied with flow-through seawater (~1 l min^{-1}) pumped from a depth of ~5 m in the adjacent embayment, Logy Bay, and hereafter termed 'ambient seawater' (or the equivalent). Ambient seawater in the latter tanks and in the experimental mesocosm with ambient seawater (see Section 2.2) therefore exhibited temperature profiles similar to those of the ocean in Logy Bay. In these tanks, we exposed rhodoliths for 7 d to comparable amounts of indirect, natural light passing through 3 circular windows (1 m diameter) overlooking Logy

Bay. We removed any visible epibionts and cryptofauna from the surface of each rhodolith with a smooth nylon brush or forceps.

Andrake & Johansen (1980) marked coralline algae with Alizarin Red with no effect on growth, and many authors have since used Alizarin Red S to study growth in coralline algae, including rhodoliths (e.g. Riosmena-Rodriguez et al. 2017). On 1 September 2012, we interrupted water delivery in both tanks and lowered the volume of water to 90 l prior to adding 10 l of seawater containing 8.5 g of dissolved Alizarin Red S, yielding a final concentration of ~85 mg l^{-1} in each tank. Rhodoliths were maintained in this stain-containing seawater for 48 h at ~10°C with immersion probe coolers (1 $tank^{-1}$) (IP-35RCL; PolyScience) controlled by timers. During staining, we used a pump (Elite802; Rolf C. Hagen) to aerate the water in each tank by delivering air at 1500 cm^3 min^{-1} to prevent deoxygenation and acidification. We controlled light conditions in each tank to emulate natural photoperiod and diel fluctuations in irradiance with (1) 61 cm long, actinic fluorescent tubes (n = 2; Marine-GLO, T8, 20 W; Rolf C. Hagen) located ~10 cm above the water surface (1 tube per half section of the tank) and emitting ~20 µmol m^{-2} s^{-1} of light daily from 10:00 to 15:00 h; and (2) indirect, natural light entering the lab as described above. These actinic tubes emit mainly in the lower range (400–580 nm) of the photosynthetically active radiation (PAR) spectrum (400–700 nm). We resumed seawater flow in both tanks at the end of the staining period to eliminate residual stain in the water.

2.2. Effects of temperature and irradiance on rhodolith growth (laboratory experiment)

To test the individual and combined effects of water temperature and irradiance on rhodolith growth, we carried out 2 consecutive runs of a laboratory mesocosm experiment in which we exposed stained rhodoliths, in a fully crossed design, to 1 of 12 combinations of controlled seawater temperatures (2, 4, 7, and 10°C) and levels of irradiance (low [~0.02], intermediate [~0.11], and high [~0.27 mol photons m^{-2} d^{-1}]) (see Table 2). The 2 runs differed only in duration and presence or absence of an ambient seawater temperature treatment (see below). These temperatures fall within the typical thermal range of −1 to 16°C for shallow (<25 m deep) coastal waters in southeastern Newfoundland. Limited chilling capacity constrained our ability to test temperatures below 2°C. As with staining, we used both indirect natural lighting and direct artificial lighting from above the experimental tanks (see below) to ensure exposure of rhodoliths to daily and seasonal variation in natural light regimes, as well as to shorter wavelengths of the PAR range (400–700 nm) that predominate in shallow coastal water environments.

Each experimental run utilized 4 glass tanks (180 l; L × W × H: 120 × 30 × 50 cm) supplied with flow-through seawater (1 l min^{-1}). We arranged the tanks in a 2 × 2 grid alongside a wall of the laboratory with 2 circular windows, staggering them relative to the windows to position their right ends near one of the windows. We covered the left end of the 4 tanks with opaque canvas to block natural light penetration through that end, leaving the other sides of the 4 tanks unobstructed (no canvas). This particular arrangement, together with orientation of the windows relative to the daily trajectory of sun, created similar gradients of indirect, natural light in the 4 tanks, with progressively less light from right to left ends. We subdivided each tank in 3 sections based on visual delineation of differences in irradiance: (1) low, in the first quarter of the tank flanking the covered end; (2) intermediate, in the second quarter of the tank adjacent to the low irradiance quarter; and (3) high, in the remaining half of the tank flanking the uncovered end (Fig. 1B). Seawater entered each mesocosm by trickling gently vertically at the surface of the water, near the end of the tank facing the lab window (high irradiance section). The overflow left each mesocosm through a 2.5 cm hole located at the top of the opposite end (low irradiance section) (Fig. 1B). This arrangement resulted in very low and homogeneous water flows across the entire bottom of each mesocosm, therefore greatly limiting the likelihood that water flow interfered with the effects of irradiance on rhodoliths.

No structures in the tanks physically separated rhodoliths and water among sections, and we lit each tank with one 61 cm long, actinic fluorescent tube (Marine-GLO, T8, 20 W; Rolf C. Hagen, also used for staining) located ~10 cm above the water surface in the high irradiance section and emitting light daily from 10:00 to 15:00 h (Fig. 1B). The actinic fluorescent tube contributed on average ~1, 5, and 14 µmol photons m^{-2} s^{-1} to total irradiance in the low, intermediate, and high irradiance sections, respectively, as measured in the dark, prior to the onset of the experiment, with a PAR meter (LI-250A; LI-COR) fitted to an underwater quantum sensor (LI-192; LI-COR). We randomly assigned each tank to 1 of the 4 temperature treatments. We also set up a fifth tank at the margin of the 2 × 2 grid, which was supplied with

ambient seawater and recreated the same light environment as in the other 4 tanks. Therefore, the only difference between this tank with ambient seawater and the other 4 tanks with controlled seawater temperatures was that the former experienced Logy Bay's daily and seasonal variation in sea temperature throughout the experiment.

The first experimental run began on 4 September 2012, when we uniformly distributed 12 stained rhodoliths on the bottom of each section in each of the 4 mesocosms, for a total of 36 rhodoliths per mesocosm with similar light exposure (Fig. 1B). The 2, 4, and 7°C treatments were gradually cooled from the 10°C onset temperature at slightly different rates: (1) 2°C: 2°C wk^{-1} for 4 wk; (2) 4°C: 2°C wk^{-1} for 3 wk; (3) 7°C: 1°C wk^{-1} for 3 wk to reduce the likelihood of thermal shock. All mesocosms were continuously supplied with seawater at 4°C from a main chilled reservoir. Temperature was maintained with 300 W water heaters (Fluval M300; Rolf C. Hagen) in the 7 and 10°C mesocosms, and with immersion probe coolers (IP 35RCL; PolyScience) in the 2°C mesocosm.

We sought to characterize temporal variation in rhodolith growth. Accordingly, we removed 3 rhodoliths from each section of each mesocosm every 3 mo (Table 1) for growth measurement (see Section 2.4). Once a month, we carefully inspected the surface of each rhodolith and removed any visible epibionts with a smooth nylon brush. On these occasions, the remaining rhodoliths were randomly overturned and assigned different locations within their respective irradiance treatment section. We terminated the first experimental run on 30 August 2013, after a total duration of 361 d. Available resources limited us to 1 mesocosm for each temperature treatment.

Table 1. Rhodolith collection dates for the laboratory (Section 2.2) and field (Section 2.3) experiments

Experiment	Collection	Date	Experimental day
Laboratory (First run)	1	1 December 2012	89
	2	1 March 2013	179
	3	2 June 2013	272
	4	30 August 2013	361
Laboratory (Second run)	1	30 November 2013	89
Field	1	3 December 2012	65
	2	10 January 2013	103
	3	2 March 2013	154
	4	2 April 2013	185
	5	27 May 2013	240
	6	17 July 2013	291
	7	29 August 2013	334
	8	17 October 2013	383

The second experimental run was carried out to account for possible confounding of temperature and mesocosm effects. It ran for 89 d, from 3 September to 30 November 2013, with the 2, 4, 7, and 10°C temperature treatments assigned to different mesocosms within the 2 × 2 grid. Our main chilling unit broke down and could not be replaced, which prevented running this run over a longer period of time. Mesocosms had no effects on rhodolith growth as indicated by post hoc pairwise comparisons that showed no differences in rhodolith growth between the 2 experimental runs after 89 d for any of the 12 combinations of temperature and irradiance levels. Collection, staining, and acclimation of rhodoliths to temperature treatments followed the protocol described above for the first experimental run. The second run did not include a fifth mesocosm with ambient seawater because it was impossible to replicate the same ambient temperature regime as in the first run. Growth measured under the 4 controlled temperature treatments in the first and second experimental runs was compared to that in the mesocosm with ambient seawater temperature of the first run.

Throughout both runs of the experiment, 2 temperature and light loggers (HOBO Pendant; Onset Computer) placed horizontally in the center of the low and high irradiance sections (1 logger per section) recorded water temperature and downwelling illuminance every 5 min at the bottom of each mesocosm. A 5 d preliminary trial during which we recorded temperature and illuminance in the 3 irradiance sections of 1 mesocosm showed (1) similar temperature in the 3 sections; and (2) 31% illuminance in the intermediate irradiance section relative to that in the high irradiance section. Accordingly, we estimated illuminance throughout the experiment in the intermediate irradiance section of each mesocosm by multiplying illuminance values in the high irradiance section by 0.31.

2.3. Growth along a depth gradient (field experiment)

We carried out a field experiment to monitor growth of stained rhodoliths held at depths of 8, 15, and 25 m in the rhodolith bed at St. Philip's. These depths correspond roughly to the shallow, middle, and deep sections of the bed, respectively (Gagnon et al. 2012, Millar & Gagnon 2018). Expected sea temperature and

irradiance decreases from shallow to deep sections presumably yielded increasingly less favorable conditions for rhodolith growth. We set the duration of the field experiment to ~12.5 mo (383 d) to capture potential seasonal differences in growth over at least 1 yr.

Three dome-shaped cages held rhodoliths at each depth (9 cages in total). Each cage consisted of a roughly circular metal ring (25 cm in diameter) topped by a semi-circular metal arch (15 cm at the highest point), both fully covered in tightly stretched nylon netting with 2 cm mesh (Fig. 1C). A 15 kg concrete block placed horizontally on the rhodolith bed anchored the bottom (circular metal ring) of each cage, whereas 3 small buoys held the top (semi-circular arch) cage upright (Fig. 1D). The 3 cages at each depth were located ~5 m from one another. This particular set-up (1) minimized alteration of natural light and water flow passing through cages; and (2) continuously maintained the bottom of the cages ~50 cm above the bed, greatly limiting benthic grazer access.

To facilitate installation on the rhodolith bed, we preassembled cages and their rhodolith content in the laboratory 3 d prior to the start of the experiment. We added 16 stained rhodoliths to each cage through a collapsible section of the netting, and attached each rhodolith to the bottom with fishing line to prevent movement and physical contact among them (Fig. 1C,D). The attachment process distributed rhodoliths evenly on cage bottoms, thus ensuring similar access to light and exposure to other environmental influences among individuals. Attachment of rhodoliths took less than 10 min per cage and was completed in a cool, moist, dim environment to limit emersion stress in rhodoliths. We submerged and maintained cages with their attached rhodoliths in large (330 l) holding tanks supplied with ambient seawater (~1 l min^{-1}) until transportation to the study site. Caged rhodoliths in those tanks were exposed to indirect, natural light passing through the same 3 circular windows of the laboratory described in Section 2.1.

The experiment began on 30 September 2012, when we removed caged rhodoliths from the flow-through holding tanks and transported them in seawater-filled containers to install them at 3 experimental depths in the rhodolith bed in St. Philip's. Approximately every 1.5 mo thereafter, divers removed 2 rhodoliths from each cage at each depth and placed them in prelabeled plastic bags, which were transported to the OSC for growth measurement (see Section 2.4). On each collection day, cages were cleaned and the temperature/light loggers were replaced by cleaned ones to prevent any biofouling from interfering with light penetration inside the cages or with logger measurements. We applied these precautions despite insignificant biofouling at each of our visits. Limited scuba bottom time prevented rearranging rhodoliths within each cage after each collection. We terminated the experiment on 17 October 2013 (383 d after it commenced), with collection of the last rhodoliths in all cages. In total, we completed 8 rhodolith collections at 15 and 25 m depths, between December 2012 and October 2013 (Table 1). A storm damaged the cages and destroyed all rhodoliths at 8 m in January 2013, yielding only 2 rhodolith collections at that depth. One temperature and light logger (HOBO Pendant; Onset Computer), attached horizontally to the top of 1 of the 3 cages with the light sensor oriented towards the sea surface, recorded sea temperature and downwelling illuminance at each depth every 5 min throughout the experiment.

2.4. Growth measurement

Growth in branched rhodoliths can be measured as the thickness of new layers of calcified tissue added at the apices of branches since marking (Blake & Maggs 2003, Darrenougue et al. 2013). We used the same protocol to measure branch elongation in rhodoliths from the laboratory mesocosm and field experiments. Following oven drying at 40°C for 48 h, we filed down, for each rhodolith, 10 haphazardly chosen branch tips (distal ends) to their center with a precision rotary tool (3000; Dremel) fitted with a 240-grit sanding disc. We then gently broke off the filed tips, hand-polished them with 600-grit sandpaper to expose stain marks, and photographed them at 40× magnification with a microscope equipped with a digital camera (BA300; Motic). Digital photographs and image analysis software (Motic Images Plus 2.0) were used to measure branch elongation in each filed tip, defined as the maximum axis length between the stain mark and apex of the branch (Fig. 1E). We then calculated mean rhodolith branch elongation, hereafter referred to as growth, by averaging the 10 branch elongation measurements.

2.5. Light conversion

Our light loggers for the laboratory and field experiments measured illuminance, in lux (lx), between 150 and 1200 nm. To compare results among the lab and field experiments and published studies, we converted all illuminance values to PAR equivalents (referring to the segment of the electromagnetic

spectrum between 400 and 700 nm used for most photosynthesis) with the following procedures derived from Long et al. (2012):

$$\mathrm{PAR} = \frac{I}{\mathrm{CF}} \quad (1)$$

where PAR is in µmol photons m^{-2} s^{-1}, I is illuminance in lux (lx), and CF is a lux to PAR conversion factor in lx (µmol photons m^{-2} s^{-1})$^{-1}$ obtained from simultaneous measurement of illuminance and irradiance for artificial actinic light in the mesocosms (low irradiance section = 14.7, intermediate = 18.1, and high = 22.1) and sunlight in the field at 8, 15, and 25 m depths (23.4) (see Tables S1 & S2, Methods 1, Supplement 1 at www.int-res.com/articles/suppl/m663p077_supp.pdf). For the laboratory mesocosm experiment, we used actinic light conversion factors to convert illuminance data acquired each day between 10:00 and 15:00 h, when artificial light provided most of the irradiance, and a sunlight conversion factor for illuminance data acquired between 15:05 and 09:55 h, when lights were off. Logistical considerations prevented establishing a conversion factor for sunlight in the mesocosms during the experiment. Accordingly, we applied a conversion factor for sunlight in the field (23.4) to all mesocosm illuminance data measured in the absence of actinic light.

We calculated daily light integral (DLI), a time-integrated irradiance (PAR) integral indicating the amount of photosynthetically active photons received by a given surface over 24 h (Korczynski et al. 2002), for the low, intermediate, and high irradiance treatments in the laboratory mesocosm experiment on each of the 361 and 89 d of the first and second experimental runs, respectively. We also calculated DLI in the field experiment for each of the 3 depths on each of the 383 d that the experiment lasted with the following equation (adapted from Korczynski et al. 2002):

$$\mathrm{DLI} = \sum_{i=1}^{288} \frac{300 x_i}{10^6} \quad (2)$$

where DLI is in mol photons m^{-2} d^{-1}, 288 denotes the number of PAR readings over 24 h, x_i refers to the i^{th} PAR value in µmol photons m^{-2} s^{-1}, 300 is the number of seconds separating 2 consecutive readings (1 reading every 5 min), and 10^6 is the µmol to mol scaling factor.

2.6. Thermal and irradiance indices

We used 1 thermal index, degree-day (DD), and 1 irradiance index, PAR-day (PD), to examine the relationship between rhodolith growth and the changing thermal and light environments in the field, and in particular the relative importance that these variables have in controlling rhodolith growth. If rhodolith growth scales positively with temperature and/or irradiance, then the accumulation of new tissue layers at the distal end of a growing branch should vary proportionally with the rate of accumulation of DD and/or PD.

2.6.1. DD

DD is an index of heat accumulation used in marine ecological studies to link distributional patterns and biological processes to the thermal environment (Scheibling & Gagnon 2009, Alahuhta et al. 2011, Beck et al. 2014). In the present study, DD was used to determine the extent to which rhodolith growth was related to intra-annual variation in sea temperature at depths of 15 and 25 m (field experiment). DD, which is the sum of daily mean water temperatures (DMWTs) over a given period of time since the onset of the field experiment, was calculated with the following equation for each of the 8 days on which rhodoliths were collected, and their growth subsequently measured:

$$\mathrm{DD}_k = \sum_{i=1}^{k} \mathrm{DMWT}_i \quad (3)$$

where DD is in °C, k is the number of days elapsed between the onset of the experiment and a given rhodolith collection day, and DMWT_i is the i^{th} DMWT in °C.

2.6.2. PD

PD is an index of DLI accumulation used in the present study to determine the extent to which rhodolith growth was related to intra-annual variation in irradiance at depths of 15 and 25 m (field experiment). PD, which is the sum of DLI values over a given period of time since the onset of the field experiment, was calculated with the following equation for each of the 8 days on which rhodoliths were collected, and their growth subsequently measured:

$$\mathrm{PD}_k = \sum_{i=1}^{k} \mathrm{DLI}_i \quad (4)$$

where PD is in mol photons m^{-2} d^{-1}, k is the number of days elapsed between the onset of the experiment and a given rhodolith collection day, and DLI_i is the i^{th} DLI value in mol photons m^{-2} d^{-1}. DD and PD were

not calculated for the experimental depth of 8 m because the interrupted growth time series at this depth (see Section 2.3) prevented testing the relationship between continuous accumulation of rhodolith tissue (growth) and rates of temperature and irradiance accumulation over the entire experiment.

2.7. Statistical analysis

We used linear mixed-effects models (LMMs) to examine individual and interactive treatment effects on rhodolith growth in our laboratory and field experiments. All LMMs included fixed, random, and nested factors to properly handle the dependency structure of the data (see Supplement 2 for a detailed discussion of how we implemented the dependency structures for both experiments). For each term in our model, we calculated an *F*-ratio based on correct allocation of the expected mean squares that form the *F*-ratio denominator (Quinn & Keough 2012; Supplement 2).

2.7.1. Laboratory mesocosm experiment

We used 1 LMM (split-plot ANCOVA; Quinn & Keough 2012) to compare rhodolith growth rates among controlled temperature and irradiance treatments (n = 180), with the fixed, between-plots factor Temperature (the 4 water temperature treatments: 2, 4, 7, and 10°C); random factor Mesocosm (each of the 8 experimental mesocosms) nested within Temperature (2 mesocosms per temperature treatment; 1 in each of the 2 experimental runs); fixed, within-plots factor Irradiance (the 3 irradiance treatments: low, intermediate, and high); and covariate Time (number of days elapsed since the onset of the experiment). We tested for homogeneity of the regression slopes of rhodolith growth as a function of time (i.e. growth rate) among the various combinations of Temperature and Irradiance treatments. Accordingly, we considered the significance of the Temperature × Time, Irradiance × Time, and Temperature × Irradiance × Time interaction terms (Quinn & Keough 2012) (Table S3, Supplement 2). We implemented a power of the variance covariate structure to account for the increasing variance in rhodolith growth over time (Zuur et al. 2009). We used pairwise slope comparison (*t*-test) to compare growth rates in the low, intermediate, and high irradiance sections of the mesocosm with ambient seawater temperature (n = 12 for each irradiance treatment) with those from the corresponding irradiance sections of the mesocosms with controlled seawater temperatures (2, 4, 7, and 10°C) (n = 15 for each controlled temperature and irradiance combination).

2.7.2. Field experiment

We used 1 LMM (nested ANCOVA) with the fixed factor Depth (8, 15, and 25 m); random factor Cage (each of the 9 cages) nested within Depth (3 cages per depth); and covariate Time (number of days elapsed since the onset of the experiment) to compare rhodolith growth rates among depths (n = 36) during the first 103 d of the experiment, i.e. before the storm destroyed rhodolith cages at 8 m (see Section 2.3). This statistical approach is similar to that of the laboratory experiment as we tested for homogeneity of the regression slopes of rhodolith growth as a function of time among the various experimental depth treatments, considering the Depth × Time interaction (Quinn & Keough 2012) (Table S4, Supplement 2).

Non-linear growth patterns over time at 15 and 25 m over the full duration (383 d) of the experiment (see Section 3) prevented using the ANCOVA approach to compare growth rates among the 2 depth treatments. Instead, we used an LMM (2-way nested ANOVA; Quinn & Keough 2012) experimental design with the fixed factors Time (the 8 rhodolith collection events) and Depth (15 and 25 m), and random factor Cage (each of the 6 cages) nested within Depth (3 cages per depth) to compare rhodolith growth between the 2 uninterrupted growth time series at 15 and 25 m and among the 8 rhodolith collections (n = 96) (Table S5, Supplement 2). We implemented an identity variance to account for different variances in rhodolith growth among rhodolith collections (Zuur et al. 2009). All analyses were applied to raw (non-transformed) data.

To determine whether the observed intra-annual variation in rhodolith growth in the field (see Section 3) was best explained by seasonal variation in thermal (DD) and/or irradiance (PD) indices (see Section 2.6 for details on both indices), we used 4 LMMs, each with the fixed factor Depth (15 or 25 m), random factor Cage (each of the 6 cages) nested within Depth (3 cages per depth) and either or both indices as covariates (with or without their interaction) (Table S6, Supplement 2). We compared Akaike's information criterion (AIC) of the 4 models to identify the model with the best fit (the lower the AIC, the better the fit of the model; Zuur et al. 2009). We implemented a

power of the variance covariate to all models to account for the increasing variance in rhodolith branch elongation with increasing DD and PD.

All LMMs with 2 or more fixed factors included all fixed factor interaction terms as well as all fixed factor × covariate interaction terms. We verified linearity, homogeneity of variance, and normality of the residuals by examining the distribution of the residuals and the normal probability plot of the residuals, respectively (Snedecor & Cochran 1994). We used paired *t*-test comparisons to detect differences among levels within a factor (ANCOVAs and ANOVA), and to compare growth estimates obtained in the mesocosm with ambient seawater temperature to those from the mesocosms with controlled seawater temperatures. All analyses were carried out with R v. 3.6.1 (R Core Team 2019), using a significance level of 0.05. Rhodolith annual growth reported for the laboratory experiment describes model-predicted values at Time = 365 d (number of days in a year) assuming no growth at the onset of the experiment (i.e. intercepts corrected to 0).

3. RESULTS

3.1. Laboratory mesocosm experiment

3.1.1. Temperature

DMWTs in the controlled temperature mesocosms differed by no more than 0.5°C (in the 10°C treatment) from the targeted temperatures during the post-acclimation period (Days 29–361) (Table 2, Fig. 2A). DMWT in the mesocosm with ambient seawater temperature averaged 6.7°C and varied more than in the controlled temperature mesocosms (Table 2, Fig. 2B); as expected, it declined seasonally from ~15.6°C at the onset of the experiment in early September 2012 to ~0.5°C in mid-February

Table 2. Mean (SD) water temperature and daily light integral (DLI) in the laboratory mesocosms for various segments of the first and second experimental runs. Temperatures for the controlled (2, 4, 7, and 10°C) and ambient mesocosms are averaged daily means (see Figs. 2 & 3 for daily mean water temperatures and DLI, respectively). NR: value is not relevant to the present study

Factor	First run			Second run
Treatment	Full run (361 d)	Post-acclimation (Days 29–361)	First 89 d	Full run (89 d)
Temperature (°C)				
2	2.6 (1.6)	2.3 (0.8)	3.4 (2.7)	3.6 (3.3)
4	4.6 (1.1)	4.4 (0.8)	5.0 (1.7)	5.3 (2.1)
7	7.4 (1.0)	7.4 (1.0)	7.3 (1.0)	7.4 (1.0)
10	10.4 (1.1)	10.5 (1.0)	10.0 (1.1)	9.9 (1.1)
Ambient	6.7 (4.7)	NR	NR	NR
Irradiance (DLI) (mol photons m^{-2} d^{-1})				
Low				
2	0.02 (0.02)	NR	0.01 (0.01)	0.01 (0.01)
4	0.02 (0.01)	NR	0.01 (0.01)	0.01 (0.01)
7	0.02 (0.01)	NR	0.01 (0.01)	0.01 (0.01)
10	0.03 (0.02)	NR	0.02 (0.01)	0.01 (0.01)
Mean (2, 4, 7,10)	0.02 (0.01)	NR	0.01 (0.01)	0.01 (0.01)
Ambient	0.03 (0.02)	NR	0.02 (0.01)	NR
Intermediate				
2	0.10 (0.02)	NR	0.08 (0.04)	0.08 (0.02)
4	0.11 (0.04)	NR	0.09 (0.04)	0.09 (0.02)
7	0.10 (0.03)	NR	0.09 (0.03)	0.10 (0.02)
10	0.11 (0.03)	NR	0.08 (0.04)	0.11 (0.03)
Mean (2, 4, 7,10)	0.11 (0.03)	NR	0.09 (0.03)	0.09 (0.02)
Ambient	0.10 (0.03)	NR	0.09 (0.04)	NR
High				
2	0.26 (0.08)	NR	0.20 (0.09)	0.22 (0.06)
4	0.29 (0.10)	NR	0.25 (0.11)	0.25 (0.05)
7	0.28 (0.07)	NR	0.24 (0.09)	0.27 (0.05)
10	0.26 (0.08)	NR	0.20 (0.09)	0.29 (0.07)
Mean (2, 4, 7,10)	0.27 (0.07)	NR	0.22 (0.09)	0.26 (0.05)
Ambient	0.27 (0.08)	NR	0.24 (0.11)	NR

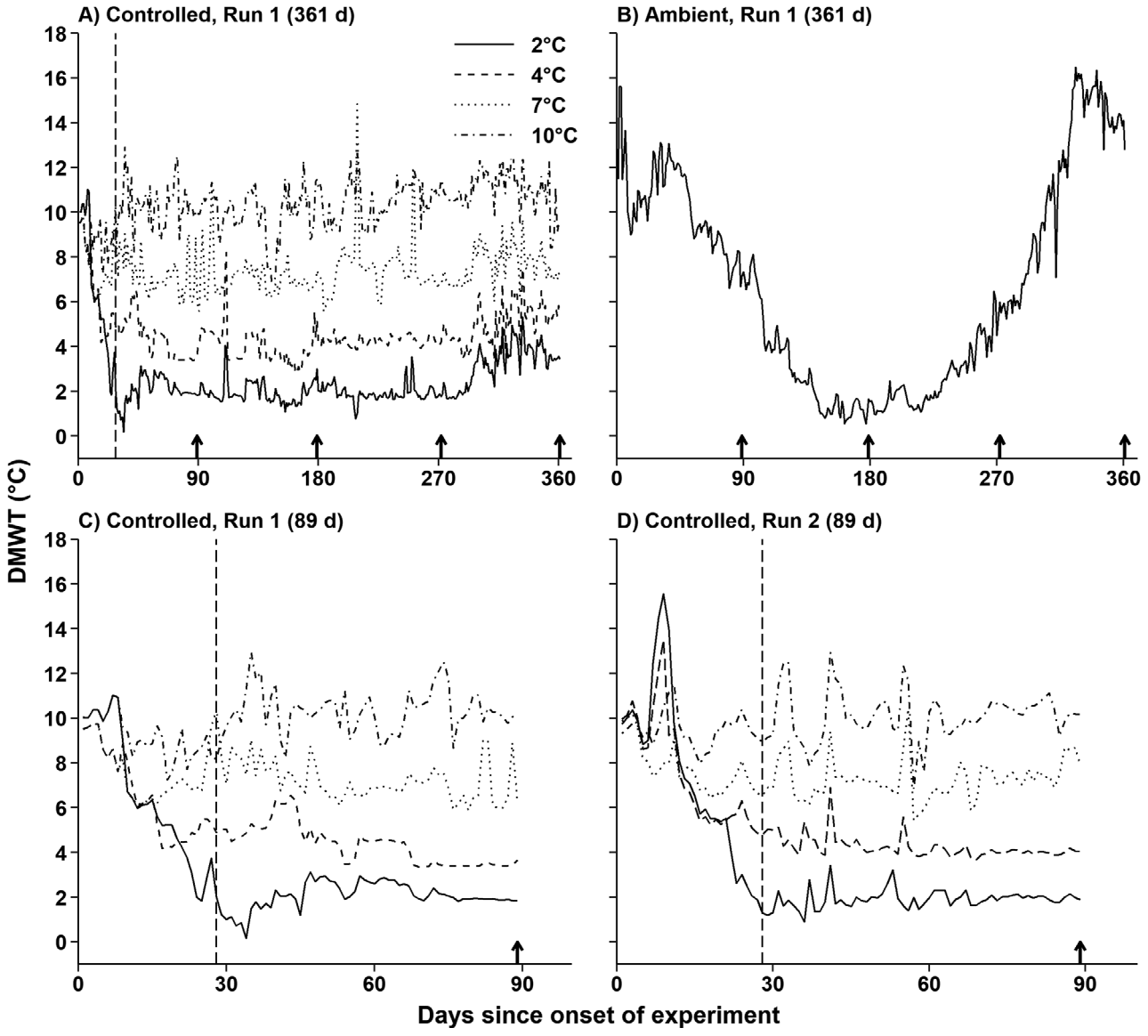

Fig. 2. Daily mean water temperature (DMWT) in (A) each of the 4 mesocosms with controlled temperature (2, 4, 7, and 10°C) throughout the first experimental run; (B) the mesocosm with ambient temperature throughout the first experimental run; (C) each of the 4 mesocosms with controlled temperature during the first 89 d of the first experimental run; and (D) each of the 4 mesocosms with controlled temperature throughout the second experimental run. The vertical dashed line in panels A, C, and D marks the end of the acclimation during which rhodoliths in mesocosms at 2, 4, and 7°C were exposed to decreasing temperatures from an initial temperature of 10°C. Arrows along abscissas mark days since the onset of both experimental runs on which 9 rhodoliths (3 per irradiance treatment) were removed from each mesocosm to determine growth (see Table 1 for collection dates)

2013, followed by an overall increase to ~16.5°C near the end of the experiment in late July 2013 (Fig. 2B). Ambient DMWT was <1°C only 3% of the time, over less than 5 consecutive days. DMWT patterns in the controlled temperature mesocosms during the first 89 d of the first experimental run were similar to those throughout the 89 d duration of the second run (Table 2, Fig. 2C,D; Fig. S1, Methods 2, Supplement 3).

3.1.2. Irradiance

At 0.27 mol photons m^{-2} d^{-1}, mean DLI throughout the first experimental run (361 d) in the high irradiance treatment was ~3 and 14 times higher than in the intermediate and low irradiance treatments, respectively (Table 2). This pattern closely resembled that during the first 89 d of the first experimental run and 89 d of the second run, with differences

in mean DLI of no more than 0.01, 0.03, and 0.09 mol photons m^{-2} d^{-1} among mesocosms in the low, intermediate, and high irradiance treatments, respectively (Table 2). Mean DLI remained fairly constant throughout both experimental runs, with smallest to largest daily fluctuations in the lowest to highest irradiance treatments, respectively (Table 2, Fig. 3A,B). Mean instantaneous irradiance (the average of all measures of irradiance at a given time of day) over the first experimental run exhibited a clear, daily cycle in all 3 irradiance treatments with (1) low (<1 µmol photons m^{-2} s^{-1}) values from 06:00 to 09:00 h, followed by (2) a 2.5 h increase to peak values (up to 15.2 µmol photons m^{-2} s^{-1} under high irradiance) that persisted from 11:30 to 14:00 h, followed by (3) a 2 h decrease to low values from 16:00

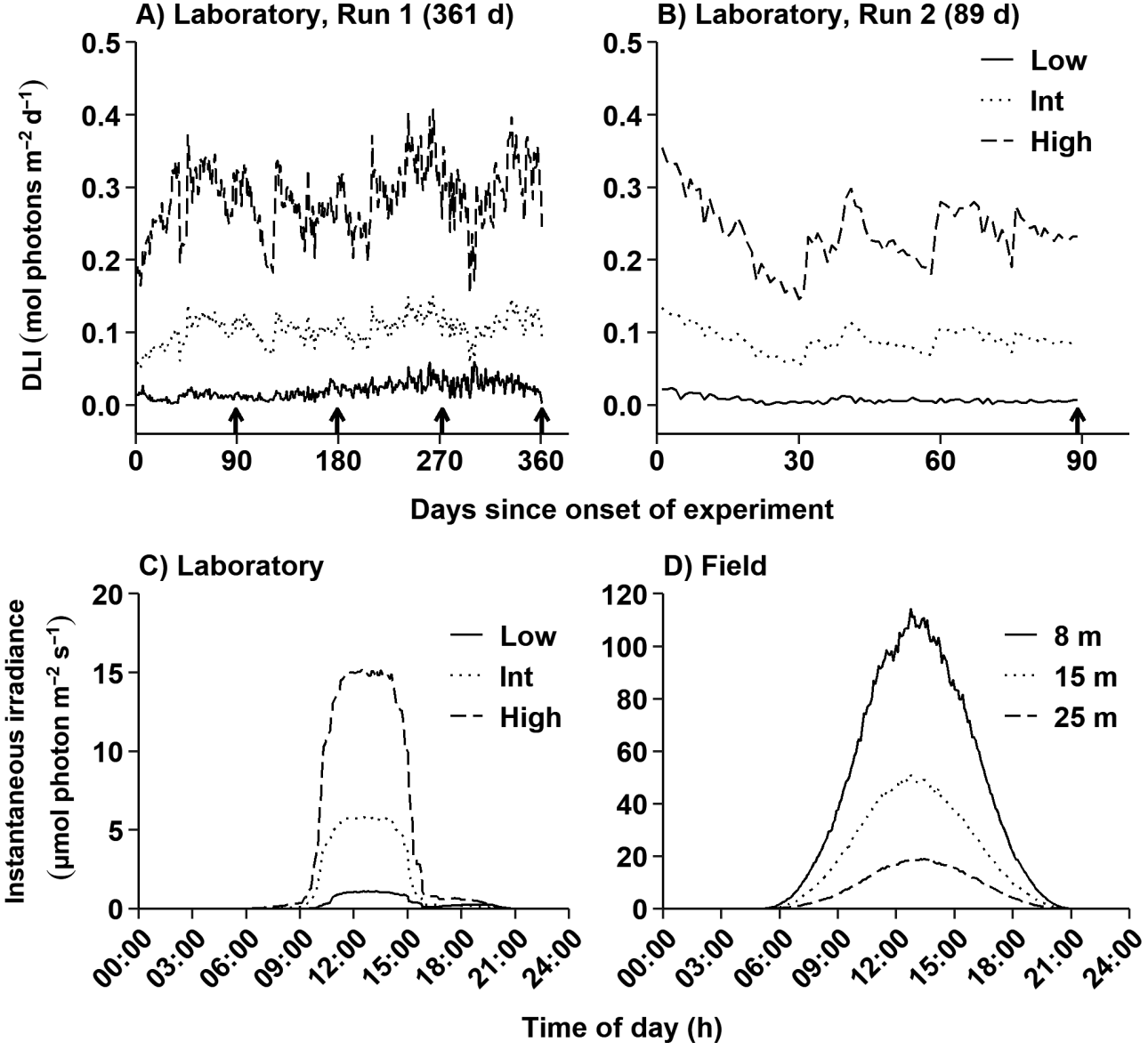

Fig. 3. Mean daily light integral (DLI, data pooled across all mesocosms) for the low, intermediate, and high irradiance treatments in the laboratory mesocosm experiment throughout the (A) first experimental run (361 d) and (B) second experimental run (89 d). Arrows along the abscissas mark days since the onset of both experimental runs on which 9 rhodoliths (3 per irradiance treatment) were removed from each mesocosm to determine growth. Mean instantaneous irradiance regimes for (C) the low, intermediate, and high irradiance treatments in the first run of the laboratory mesocosm experiment (data pooled across all mesocosms) and (D) at 8, 15, and 25 m depths in the field experiment. Each regime averages irradiance measured every 5 min throughout the first run of the laboratory experiment (C) and the 383 d field experiment (D) (note the change of scale between panels C and D; see Table 1 for collection dates)

to 20:30 h, ending with (4) nearly complete darkness until 06:00 h the next day (Fig. 3C). Mean instantaneous irradiance during the peak period in the high irradiance treatment was 3 and 13 times higher than in the intermediate and low irradiance treatments, respectively (Fig. 3C).

3.1.3. Rhodolith growth

There was no interactive effect of temperature and irradiance on rhodolith growth. Growth was ~20% lower at 10°C (96 ± 4 [95%CI] µm) than at 4°C (122 ± 5 µm) and 7°C (123 ± 4 µm) during the 89 d separating the onset of the laboratory experiment and the first rhodolith collection (Fig. 4A; Table S7, Supplement 4). Growth then stabilized for the rest of the experiment, increasing linearly at similar rates in all temperature treatments (Table 3, Fig. 4A; Table S7, Supplement 4). Mean branch tip elongation after 361 d (end of the experiment) was between 2.4 (at 7°C) and 4.6 (2°C) times higher than after 89 d (first growth measurement) (Fig. 4A).

Table 3. Summary of regression coefficients of the spit-plot ANCOVA in the laboratory experiment, and nested ANCOVA in the field experiment (both applied to raw data) examining the relationships between rhodolith (*Lithothamnion glaciale*) growth and time elapsed since the onset of the 361 d laboratory mesocosm experiment at the various water temperatures and irradiances tested, and between the onset of the field experiment and the second rhodolith collection (103 d) at the 3 experimental depths

Experiment Factor/level	N	Intercept (SE)	Slope (SE)
Laboratory experiment (controlled temperature)			
Temperature (°C)			
2	45	68.95 (13.18)	0.44 (0.05)
4	45	76.27 (14.29)	0.50 (0.05)
7	45	88.48 (16.22)	0.44 (0.05)
10	45	69.55 (14.29)	0.38 (0.05)
Irradiance			
Low	60	78.80 (10.19)	0.33 (0.05)
Intermediate	60	85.02 (10.06)	0.34 (0.05)
High	60	64.63 (11.63)	0.65 (0.05)
Laboratory experiment (ambient temperature)			
Irradiance			
Low	12	76.24 (21.90)	0.34 (0.09)
Intermediate	12	77.41 (40.89)	0.36 (0.17)
High	12	59.18 (34.12)	0.68 (0.14)
Field experiment (Collections 1 & 2)			
8 m	12	30.7 (19.0)	0.68 (0.22)
15 m	12	19.7 (35.8)	1.39 (0.42)
25 m	12	77.0 (27.0)	0.94 (0.31)

Contrary to temperature, the rate of change in rhodolith growth differed significantly among the 3 irradiances tested (Table S7, Supplement 4); it was twice as high at high than at low or intermediate irradiances (Table 3, Fig. 4B). Branch tips after 361 d were between 2.8× (low irradiance) and 4.5× (high irradiance) longer than after 89 d (Fig. 4B). Annual growth rate did not differ significantly among the 4 controlled temperature treatments, ranging from 139 ± 18 (CI) µm yr^{-1} (at 10°C) and 183 ± 18 µm yr^{-1} (at

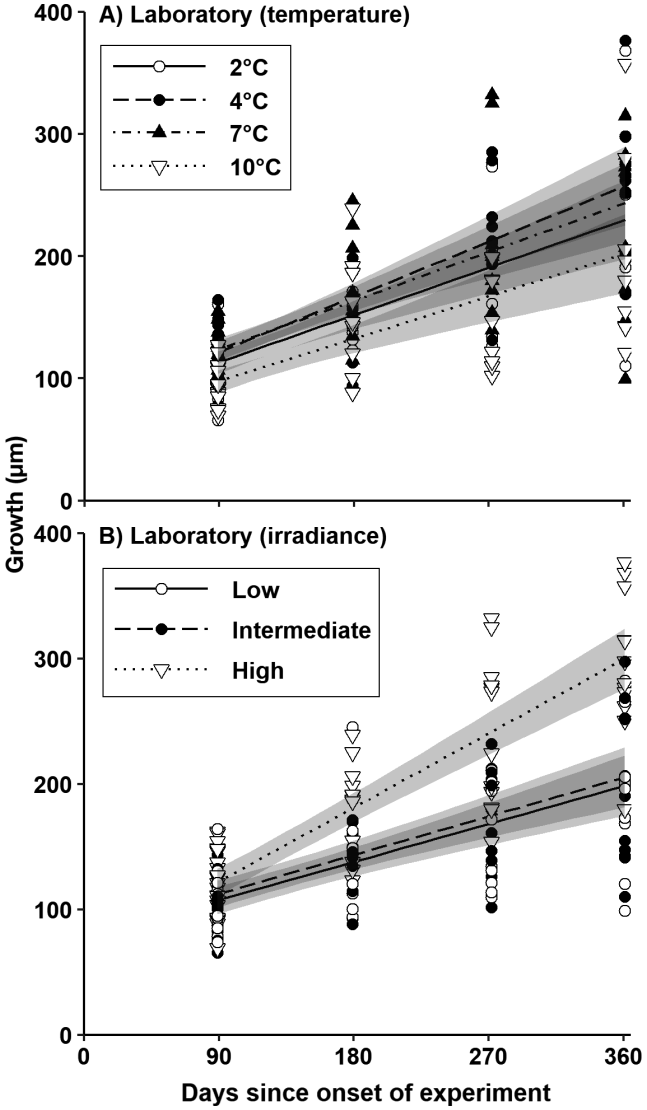

Fig. 4. Relationship between rhodolith (*Lithothamnion glaciale*) growth (±95% CI) and number of days elapsed since the onset of the laboratory experiment for (A) each of the 4 controlled water temperatures tested (data pooled across the first and second experimental runs and irradiance treatments; n = 45 for 2, 4, 7, and 10°C] and (B) each of the 3 irradiances tested (data pooled across the 2 experimental runs and controlled temperature treatments; n = 60 for each irradiance)

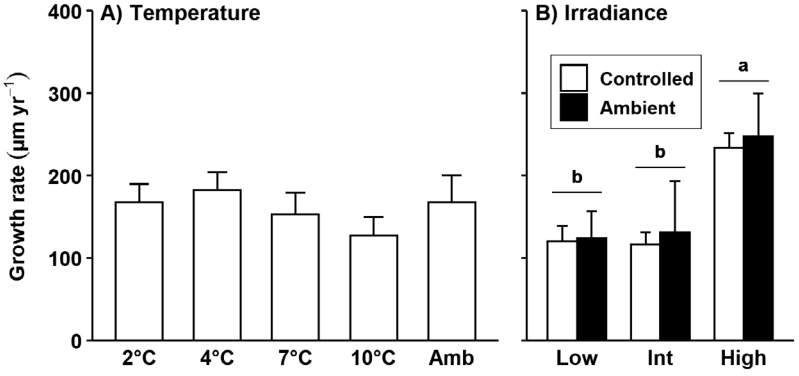

Fig. 5. Annual growth rate (+95% CI) of rhodoliths (*Lithothamnion glaciale*) at the (A) 4 controlled and 1 ambient (Amb) water temperatures (data pooled across irradiances) and (B) 3 irradiances for the controlled (data pooled across temperatures) and ambient water temperatures tested in the laboratory experiment. Growth rates at ambient temperature are compared to those at the controlled temperatures (A), and to those at each irradiance (B). Annual growth rates are model predictions at Time = 365 d assuming null growth at Time = 0. Bars connected with horizontal lines are not statistically different. Pairs of bars not sharing the same letters differ statistically (paired *t*-test; $p < 0.05$)

4°C), yet it was nearly 2× higher at high (237 ± 18 µm yr^{-1}) than at low (120 ± 18 µm yr^{-1}) or intermediate (124 ± 18 µm yr^{-1}) irradiances (Fig. 5). Growth rates of rhodoliths exposed to ambient seawater temperature in the low (124 ± 29 µm yr^{-1}), intermediate (131 ± 29 µm yr^{-1}), and high (248 ± 51 µm yr^{-1}) irradiance treatments were similar to those of rhodoliths exposed to the controlled temperature treatments (Fig. 5; Table S8, Supplement 4).

3.2. Field experiment

3.2.1. Temperature

DMWT differed among treatment depths (6.7 ± 5.3 [SD], 6.1 ± 4.7, and 4.5 ± 3.8°C at 8, 15, and 25 m, respectively) throughout the 383 d field experiment. DMWT varied similarly at 8, 15, and 25 m depths during the first ~5 mo of the field experiment, steadily decreasing from ~12°C in early October 2012 to a minimum of ~ −0.4°C by late February 2013 (Fig. 6A–C). DMWT generally increased at all depths during the remainder of the experiment, although at an increasingly lower and more variable rate with increasing depth, resulting in mean temperature differences among the 3 depths (Fig. 6A–C). It peaked at all depths between early August and October 2013, to 17.1, 15.9, and 13.2°C at 8, 15, and 25 m, respectively (Fig. 6A–C). These patterns suggest that a thermocline developed over spring and summer that kept the shallowest (8 m) rhodoliths in a warmer and more stable thermal environment than deeper (15 and 25 m) rhodoliths (Fig. 6A–C).

3.2.2. Irradiance

Like temperature, mean irradiance throughout the field experiment decreased non-linearly with increasing depth, with 55% higher irradiance at 8 m (2.7 ± 3.0 [SD] mol photons m^{-2} d^{-1}) than at 15 m (1.2 ± 1.3 mol photons m^{-2} d^{-1}) and 58% higher at 15 than at 25 m (0.5 ± 0.6 mol photons m^{-2} d^{-1}) (Fig. 6D–F). During the first ~5 mo (October 2012 to February 2013), irradiance remained consistently low, <2.6 mol photons m^{-2} d^{-1} at all depths, followed by a brief increase (up to 2 times higher at 8 m) in March 2013 (Fig. 6D–F). Irradiance at all depths decreased to low levels for a few weeks in April (most likely as a result of the annual phytoplankton bloom), then increased markedly (more so at 8, than at 15 and 25 m) over the remainder of spring and early summer (Fig. 6D–F). It peaked at all depths in June or July 2013, to 13.0, 6.1, and 3.5 mol photons m^{-2} d^{-1} at 8, 15, and 25 m, respectively (Fig. 6D–F). Mean daily peak irradiance at 8 m was ~2 and 6 times higher than at 15 and 25 m, respectively (Fig. 3D). Daily irradiance patterns were similar in the field and laboratory experiments, although peaks at 8, 15, and 25 m depths were ~8, 9, and 17 times higher than in the high, intermediate, and low irradiance treatments, respectively (Fig. 3C,D).

3.2.3. Rhodolith growth (overall)

Rhodolith growth was ~30–45% lower at 8 (75 µm) than at 15 (110 µm) and 25 m (138 µm) depths between the onset of experiment and the first rhodolith collection 65 d later (Fig. 7A; Table S9, Supplement 4). Growth then stabilized over the following 38 d that separated the first and second rhodolith collections, increasing at similar rates among depths (Fig. 7A; Table S9, Supplement 4). Mean branch tip elongation after 103 d was between 26% (at 25 m) and 49% (at 15 m) higher than after 65 d (Figs. 6G–I & 7A). For the 383 d uninterrupted time series at 15 and 25 m, growth was similar between depths but varied similarly among collection events at both depths (Fig. 7B; Table S9, Supplement 4), and was more than 2 times higher at

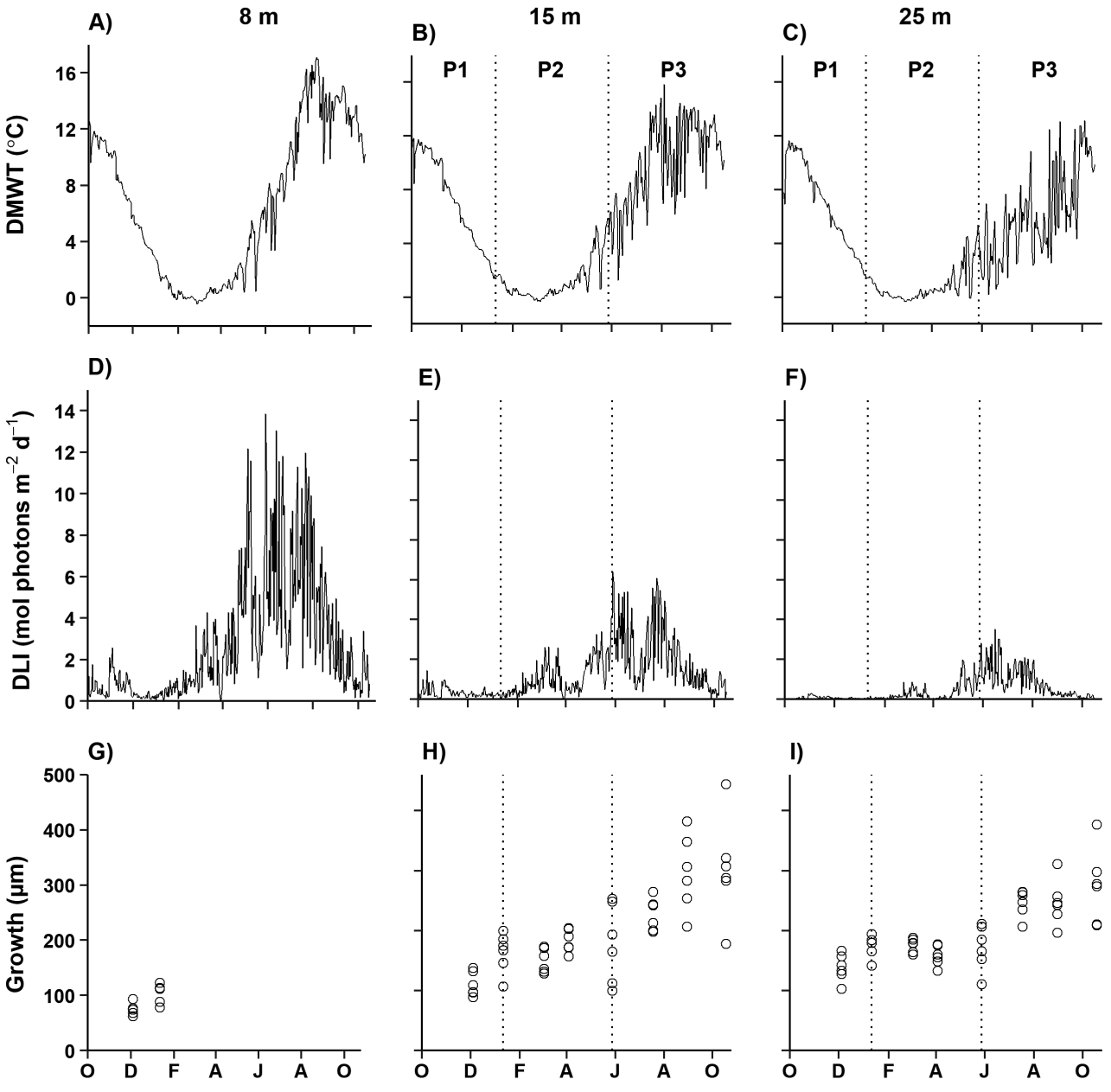

Fig. 6. (A–C) Daily mean water temperature (DMWT), (D–F) daily light integral (DLI), and (G–I) growth of rhodoliths (*Lithothamnion glaciale*) at 8, 15, and 25 m depths during the 383 d field experiment. Vertical dotted lines separate 3 main growth phases: Phase 1 (P1) and Phase 3 (P3), which denote positive growth, and Phase 2 (P2), which denotes arrested growth (see Sections 2.3 and 2.6.2 for experimental details and calculation of DLI). Letters along abscissas indicate months, from October 2012 to October 2013

383 d (end of experiment; 289 ± 21 [95%CI] µm) than at 65 d (first rhodolith collection; 124 ± 7 µm) (Fig. 7B).

3.2.4. Rhodolith growth (seasonal phases)

Rhodolith growth pooled across the 15 and 25 m depths increased by 36% during the 38 d that separated the first and second rhodolith collections (Phase 1) and remained remarkably stable (Phase 2) during the following 137 d (i.e. until the fifth collection, Fig. 7B). Growth then resumed and increased (Phase 3) by 35%, and 22% within each time block separating, respectively, the fifth and sixth (51 d), and sixth and eighth (92 d) collections (Fig. 7B). During Phase 1 (first phase of positive

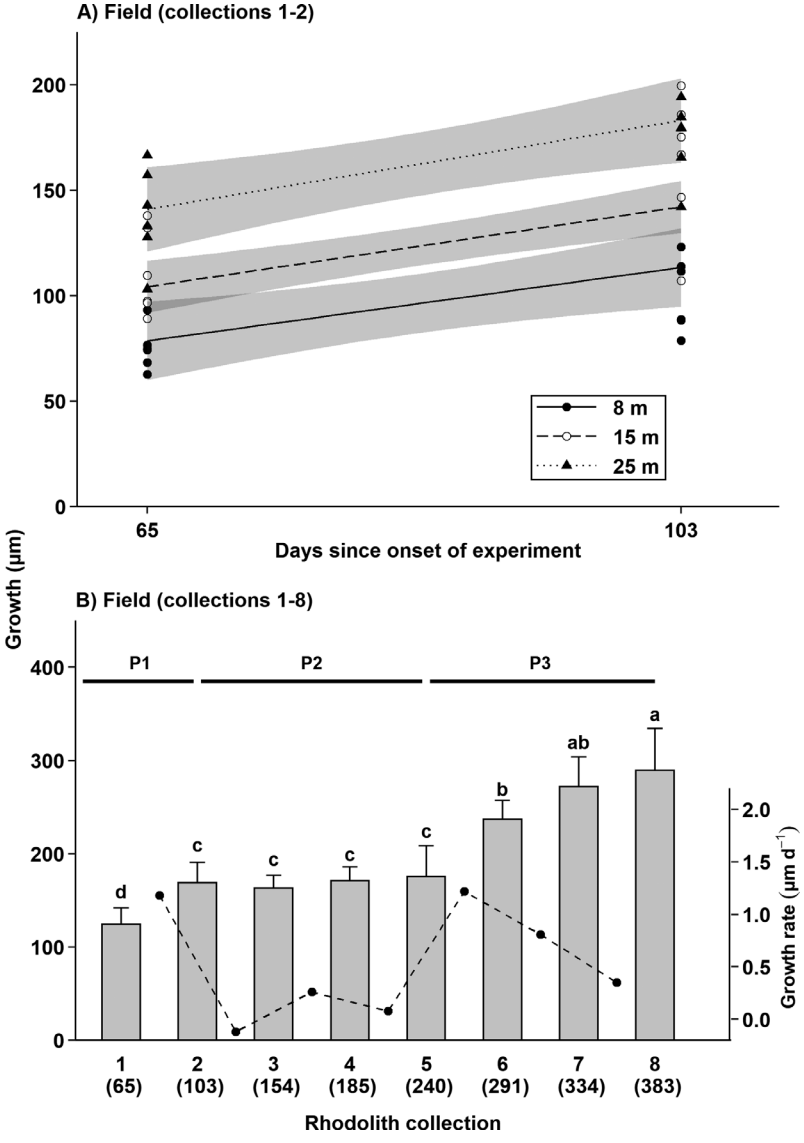

Fig. 7. (A) Relationship between rhodolith (*Lithothamnion glaciale*) growth (±95% CI) and number of days elapsed since the onset of the field experiment during the first 2 rhodolith collections when rhodoliths were present at the 3 experimental depths (n = 12 per depth). (B) Mean growth (±95% CI) (data pooled across the 15 and 25 m depths) on each of the 8 rhodolith collection events (n = 12 per collection). Solid dots connected with dashed lines show changes in mean growth rate between consecutive rhodolith collections. Numbers in parentheses under each rhodolith collection event number on the abscissa indicate the number of days elapsed since the onset of experiment. Phase 1 (P1) and Phase 3 (P3) denote periods of positive growth, whereas Phase 2 (P2) denotes a period of arrested growth (see Fig. 6 for timing of phases and Section 2.3 for a description of the experiment)

growth), DMWT decreased from ~12 to 1°C and DLI was consistently lowest, averaging 0.20 mol photons m^{-2} d^{-1} across both depths (Fig. 6B,C,E,F). During Phase 2 (nearly arrested growth), DMWT ranged between approximately –0.3 and 6°C, averaging ~1°C across depths. It remained below 0.5°C (which is the lowest water temperature attained in the mesocosm with ambient seawater temperature of the laboratory experiment) 77% of the time. DLI was ~4 times higher than during Phase 1, averaging 0.70 mol photons m^{-2} d^{-1} across depths (Fig. 6B,C,E,F). During Phase 3 (second phase of positive growth), DMWT increased from ~5 to 16°C and was always above 0.5°C (Fig. 6B,C). DLI peaked, averaging 1.48 mol photons m^{-2} d^{-1} across depths, which was ~7 and 2 times higher than during Phase 1 and Phase 2, respectively (Fig. 6E,F). Model selection analysis indicated that PD alone best explained intra-annual variation in rhodolith growth in the field (AIC = 977.15; Fig. 8B; Table S10, Supplement 4), followed by DD alone (AIC = 982.12; Fig. 8A), PD and DD without their interaction (AIC = 984.70), and DD and PD with their interaction (AIC = 1008.42). The rate of increase in rhodolith growth with PD, which can be viewed as a proxy of light use efficiency, was 1.7 times higher at 25 (0.64 µm [mol photons m^{-2} d^{-1}]$^{-1}$) than at 15 m (0.37 µm [mol photons m^{-2} d^{-1}]$^{-1}$) (Fig. 8C).

4. DISCUSSION

Our laboratory mesocosm and field experiments showed that growth in *Lithothamnion glaciale* rhodoliths is primarily controlled by irradiance at sea temperatures between ~1 and 16°C, yet virtually ceases when temperature reaches and drops below 0.5°C. Growth rate of rhodoliths exposed in the laboratory to various combinations of temperature (ambient, 2, 4, 7, and 10°C) and irradiance (low, intermediate, and high) over ~1 yr increased at high irradiance regardless of temperature, challenging temperature–light interactive effects reported in previous studies of *L. glaciale* (Adey 1970) and *Lithophyllum margaritae* rhodoliths (Steller et al. 2007).

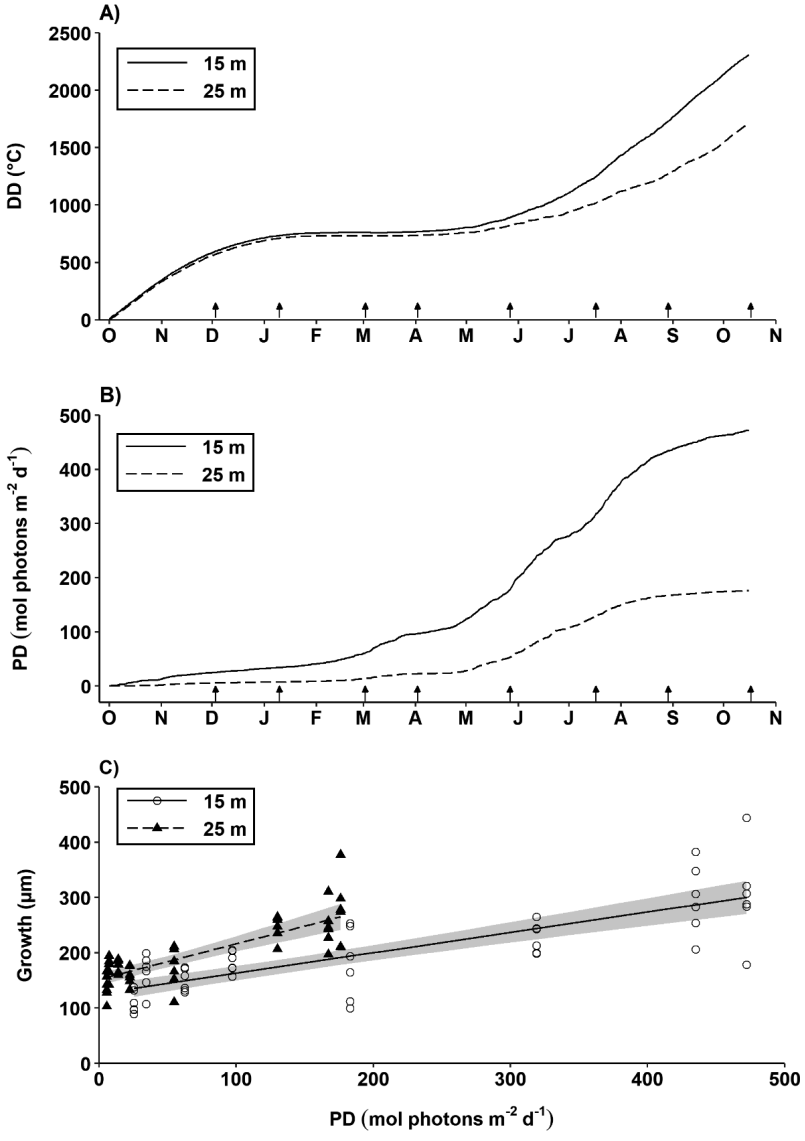

Fig. 8. (A) Degree-day (DD) and (B) PAR-day (PD) accumulation profiles at the 15 and 25 m depths during the field experiment. (C) Relationship between rhodolith (*Lithothamnion glaciale*) growth (±95% CI) and cumulated PD at the 15 and 25 m depths (n = 48 per depth). Letters and arrows along the abscissas of panels A and B indicate months and days, from October 2012 to October 2013, on which 2 rhodoliths were removed from each cage to determine growth

4.1. Temperature

Growth in rhodoliths exposed to 10°C in the laboratory experiment was significantly lower than at 2 and 4°C during the 90 d that preceded the first rhodolith collection. Possibly, growth was temporarily stimulated by a steeper thermal acclimation at the 2 lowest temperature treatments during the ~1 mo acclimation period. Adey (1970) reported transitory effects of temperature change on growth in subarctic coralline crusts, including *L. glaciale*, although contrary to the results of our laboratory experiment, growth decreased with decreasing temperature. However, rhodolith growth was unaffected by temperature in the remaining 9 mo of our laboratory experiment, averaging 161 µm yr^{-1} across the 4 controlled temperature treatments (2–10°C). These results are consistent with those of Kamenos & Law (2010), who found no difference in growth in *L. glaciale* rhodoliths grown for 1 yr at controlled temperatures between 8 and 15°C. Our finding that growth at ambient seawater temperature (168 µm yr^{-1}), which varied between ~1 and 16°C, was similar to that in the controlled temperature treatments strongly suggests that *L. glaciale* rhodoliths are largely insensitive to natural temperature variations. Our results thus extend the thermal range for relatively unimpaired growth in this species.

Several other studies support the notion that rhodoliths are generally insensitive to relatively large variation in sea temperature. For example, Bélanger & Gagnon (2020) showed linear growth in *L. glaciale* rhodoliths exposed during ~6 mo to a fairly constant light regime, albeit quite variable thermal environment oscillating between 3 and 15°C. Blake & Maggs (2003) reported no temperature effect between 10 and 18°C on growth of European *Phymatolithon calcareum* rhodoliths. Wilson et al. (2004) found no significant difference in photosynthetic activity of *P. calcareum* rhodoliths exposed to temperatures between 9 and 25°C over 4–5 wk. Steller et al. (2007) documented no significant change in net photosynthesis of Californian *Lithophyllum margaritae* rhodoliths exposed to temperatures between 10 and 30°C and irradiance <100 µmol photons m^{-2} s^{-1}. However, at ~150 µmol photons m^{-2} s^{-1}, they found that photosynthesis was ~5 times lower at 10 than 25°C, suggesting interactive effects of temperature and light above a threshold irradiance (Steller et al. 2007). In the present study, irradiance in the low, intermediate, and high irradiance treatments of the laboratory experiment was up to 2 orders of magnitude lower than the average maximum daily irradi-

ance in the field. Temperature effects on physiological processes which influence growth in *L. glaciale* rhodoliths may only occur at higher irradiance.

Studies on the effects of water temperature on metabolism show that some freshwater copepods (Epp & Lewis 1979) and rotifers (Epp & Lewis 1980) maintain constant metabolic rates within the thermal range of their natural environment, likely as a result of evolutionary adaptation to rapidly changing environments. These findings align with similar growth rates in the ambient and fixed temperature treatments of our laboratory experiment, suggesting that some coralline algae, including *L. glaciale*, are able to maintain a relatively stable metabolic rate over the temperature range of their natural habitats. Other studies, however, yielded contrasting results. For example, Martin et al. (2013) reported strong temperature-driven seasonal variation in the metabolic activity of *Lithophyllum cabiochae*. Adey (1970) measured a positive temperature effect on the marginal growth rate of several boreal and Arctic coralline species, including *L. glaciale*, until temperature exceeded thresholds beyond which growth decreased. Ichiki et al. (2000) found a >50% reduction in marginal growth in *Lithophyllum yessoense* crusts at 10 and 25°C, compared to 15 and 20°C, with no significant difference between the latter 2 temperatures, suggesting no temperature effect on growth within a certain range. Overall, temperature effects on coralline algal growth appear species specific and, in some cases, may depend on irradiance. However, the present study and that by Kamenos & Law (2010) indicated a fairly limited influence of temperature on growth in *L. glaciale* rhodoliths in the 1–18°C range.

4.2. Irradiance

Our laboratory experiment, together with the findings of other studies, provide several indications that growth in *L. glaciale* rhodoliths is chiefly driven by irradiance, with increased growth above a relatively low irradiance threshold that may correspond to the species' light compensation point. Growth in our low (~0.02 mol photons m^{-2} d^{-1}) and intermediate (~0.11 mol photons m^{-2} d^{-1}) irradiance treatments remained similarly low (~122 µm yr^{-1}), and was 2 times lower than in the high (~0.27 mol photons m^{-2} d^{-1}) irradiance treatment (~237 µm yr^{-1}). Kamenos & Law (2010) measured similar growth rates (~90–160 µm yr^{-1}) in *L. glaciale* rhodoliths exposed in the laboratory to ~5 µmol m^{-2} s^{-1} and water temperatures comparable to those in the present study. Kamenos et al. (2008) also measured similar growth rates (~146–173 µm yr^{-1}) in *L. glaciale* rhodoliths exposed in the field to temperature between ~7 and 16°C and in the laboratory to some (unspecified) ambient water temperature and light regimes.

Our laboratory experiment was not designed to specifically characterize light compensation or saturation points in *L. glaciale* rhodoliths. Nevertheless, results were consistent with (1) a compensation point of ~0.1 µmol photons m^{-2} s^{-1} in coralline red algal crusts under thick ice cover in the Antarctic Ross Sea (Schwarz et al. 2005); and (2) light saturation irradiance between ~5 and 55 µmol photons m^{-2} s^{-1} in *L. glaciale* rhodoliths (Burdett et al. 2012). Rhodoliths in our high irradiance treatment likely experienced irradiance closer to, or above, light saturation for growth, yet still below photoinhibitory levels, resulting in a higher growth rate compared to the low and intermediate irradiance treatments. We chose to explore the relationship between rhodolith growth and irradiance across a range of relatively low irradiances similar to light levels at 25 m in the field to also inform about the possible existence of an irradiance threshold below which growth is compromised. We found no evidence of a detrimental irradiance level at which growth ceased; rhodoliths in our lowest irradiance treatment grew at a relatively low (see above), yet constant rate throughout the experiment. Consistency among our findings and those of the studies described above, together with an observation by Teichert et al. (2012) that the lower distribution limit of *L. glaciale* in the Svalbard Arctic Archipelago is near ~80 m deep, where mean irradiance is only ~0.1 µmol photons m^{-2} s^{-1}, further reinforces the notion that *L. glaciale* is well adapted to low-light conditions.

Our field experiment yielded mixed conclusions about the effect of irradiance on *L. glaciale* growth. Growth during the first ~2 mo was ~40% lower at 8 (~75 µm) than at 15 and 25 m (~124 µm), but similar across the 3 depths afterwards. This finding aligns with ~50% lower growth at 5 than at 10 m depths in Irish *Phymatolithon calcareum* rhodoliths attributed to photoinhibition at the former depth (Blake & Maggs 2003). Accordingly, we propose that our observed initial, lower growth at 8 m depth was because of photoinhibition, followed by photosynthetic acclimation of low-light-adapted *L. glaciale* (Burdett et al. 2012). We also noted that on windy and wavy days, cages at 8 m swung a little more than those at 15 and 25 m. Therefore, it could also be that sloughing of epithelial cells (which contribute to growth) caused by the abrasion of rhodoliths against the mesh of the cages (to which they were attached) was

highest and above a detrimental level at 8 m, limiting growth.

Growth at 15 and 25 m was similar throughout the experiment despite a 58% decrease in irradiance at the latter depth. Schwarz et al. (2005) reported little variation in photosynthetic activity in Antarctic coralline red algal crusts at depths of 16–20 m, indicating low down-regulation of photosynthesis at irradiance below the light saturation point. Our findings that *L. glaciale* rhodolith growth was similar at 15 and 25 m depths in the field, and at low and intermediate irradiances in the laboratory experiment, yet still below growth at high irradiance in the laboratory, further support the notion that irradiance plays a key role in regulating growth in *L. glaciale* rhodoliths.

4.3. Seasonal growth phases

Our field experiment showed, for the first time, that growth in subarctic *L. glaciale* rhodoliths exhibits 3 distinct seasonal phases. The 2 phases of positive growth were when (1) sea temperature decreased from ~12 to 1°C and irradiance was consistently lowest, ~0.20 µmol photons m^{-2} s^{-1} (Phase 1: December to mid-January); or (2) sea temperature increased from ~5 to 16°C and irradiance was at least twice higher than in the 2 other phases (Phase 3: June to mid-October). These 2 phases were separated by the only phase of arrested growth (Phase 2: mid-January to end of May), when sea temperature plummeted near or below 0.5°C for 77% of the time, but irradiance was nevertheless 4 times higher than during 1 of the 2 phases of positive growth (Phase 1) and ~35 times higher than in the low irradiance treatment of the laboratory experiment under which positive growth occurred. Overall, these findings suggest an inhibitory effect of low temperature on growth.

Model selection showed that the seasonal growth pattern of *L. glaciale* rhodoliths was best explained by intra-annual variation in irradiance. The concordance between growth and irradiance was especially clear during the second phase of positive growth (Phase 3). Mean growth rate decreased from 1.20 µm d^{-1} between collections 5 and 6, to 0.82 µm d^{-1} between collections 6 and 7, and to 0.35 µm d^{-1} between collections 7 and 8, for an overall 70% decrease in growth from late May to mid-October. Mean DLI decreased by ~76% during the same period, whereas mean sea temperature increased by ~5°C. The 1.7 times higher rate of increase in rhodolith growth as a function of PD accumulation at 25 m compared to 15 m suggests a more efficient use of light by rhodoliths at greater depths, which aligns with Burdett et al. (2012), who concluded low-light adaptation in *L. glaciale* rhodoliths based on the species' photosynthetic characteristics. Adaptation to low-light environments may therefore partially explain similar growths at 15 and 25 m, despite the ~60% lower irradiance at 25 m.

Although the overall seasonal growth pattern was best explained by irradiance, correspondence between thermal indices and growth during the phase of arrested growth (Phase 2) suggests that low sea temperatures during winter interfere with *L. glaciale* growth. Adey & McKibbin (1970) found reduced or arrested growth during winter in *Phymatholithon calcareum* and *Lithothamnion corallioides* rhodoliths from Spain. However, there was no information about the thermal and light environment at the study site, preventing definitive statements about the possible effects of temperature and irradiance on growth in both species.

Our findings reinforce the notion discussed above that growth in *L. glaciale* rhodoliths is primarily controlled by irradiance at sea temperatures between ~1 and 16°C. The species appears unable to cope with prolonged exposure to low temperatures below ~0.5°C and responds to it by ceasing growth momentarily. Temperature effects may therefore override, but not interact with, those of irradiance during the coldest months of the year. Growth inhibition at low temperature has also been reported in several cold-water macroalgae (Wiencke & Dieck 1990) and coralline algae (Ichiki et al. 2000).

4.4. Conclusion and future directions

Our ~1 yr long laboratory and field experiments supported our overall hypothesis that growth in subarctic *L. glaciale* rhodoliths is chiefly controlled by irradiance, while showing some inhibitory effect of prolonged exposure to low sea temperature. Laboratory results unequivocally demonstrated that growth was unaffected by temperature between ~1 and 16°C. Our field results indicated that growth ceased at temperatures near or below 0.5°C. They also revealed that the annual growth profile of *L. glaciale* in predominantly cold subarctic waters comprises 3 dominant phases and that the switch from one phase to the next coincides with seasonal shifts in both sea temperature and light regimes. Overall, these findings (1) extend the known temperature range (~1 to at least 16°C) over which growth in *L. glaciale* rhodoliths remains unaffected; (2) identify the lower temperature limit (~0.5°C) below which growth ceases

momentarily; and (3) demonstrate that temperature effects may override, but not interact with, those of irradiance during the coldest months of the year.

L. glaciale rhodolith beds are a pervasive and dominant marine biological system in the predominantly cold waters of subarctic North Atlantic (Blake & Maggs 2003, Gagnon et al. 2012, Adey et al. 2015, Schoenrock et al. 2018). In a companion study, we showed that Newfoundland *L. glaciale* rhodoliths are somewhat resilient to low levels of infrequent increases in nutrient concentrations, yet cannot cope with prolonged exposure to modest eutrophication (Bélanger & Gagnon 2020). The present study shows that *L. glaciale* rhodoliths are nevertheless quite resilient to changes in sea temperature over a relatively broad thermal range, with sustained growth even at temperatures exceeding those normally observed during most of the year in Newfoundland coastal waters and northwards. The Arctic is warming at a rate almost twice the global average, with a clear decrease in sea-ice and ice cover that ultimately increases light availability to marine organisms (Lang et al. 2017, Bindoff et al. 2019). The present study therefore also suggests that ongoing ocean warming will benefit subarctic *L. glaciale* rhodoliths (and the highly biodiverse beds they form) by shortening the yearly period over which near-0°C sea temperatures prevent their growth. Ragazzola et al. (2016) showed alterations to the ultrastructure of *L. glaciale* exposed to high pCO_2 simulating ocean acidification. Further studies should address the vulnerability of *L. glaciale* rhodoliths to the combined effect of ongoing ocean warming and acidification and its consequences on the structure and function of Arctic and subarctic benthic communities.

Acknowledgements. We are grateful to A. P. St-Pierre and D. Frey for assistance with field and laboratory work, and to D. Schneider for statistical advice. We also thank P. Snelgrove, R. Gregory, and 3 anonymous reviewers for constructive comments that helped improve the manuscript. This research was supported by the Natural Sciences and Engineering Research Council (NSERC Discovery Grant), Canada Foundation for Innovation (CFI Leaders Opportunity Funds), Research & Development Corporation of Newfoundland and Labrador (Ignite R&D), and Department of Fisheries and Aquaculture of Newfoundland and Labrador (DFA) grants to P.G.; D.B. was supported by the Memorial University of Newfoundland President's Doctoral Student Investment Fund program.

LITERATURE CITED

Adey WH (1970) Effects of light and temperature on growth rates in boreal-subarctic crustose corallines. J Phycol 6: 269–276

Adey WH, Hayek LAC (2011) Elucidating marine biogeography with macrophytes: quantitative analysis of the North Atlantic supports the thermogeographic model and demonstrates a distinct subarctic region in the northwestern Atlantic. Northeast Nat 18:1–128

Adey WH, McKibbin DL (1970) Studies on the maerl species *Phymatolithon calcareum* (Pallas) nov. comb. and *Lithothamnium corallioides* Crouan in the Ria de Vigo. Bot Mar 13:100–106

Adey W, Halfar J, Humphreys A, Suskiewicz T, Belanger D, Gagnon P, Fox M (2015) Subarctic rhodolith beds promote longevity of crustose coralline algal buildups and their climate archiving potential. Palaios 30:281–293

Ahn JH, Grant SB, Surbeck CQ, Digiacomo PM, Nezlin NP, Jiang S (2005) Coastal water quality impact of stormwater runoff from an urban watershed in southern California. Environ Sci Technol 39:5940–5953

Alahuhta J, Heino J, Luoto M (2011) Climate change and the future distribution of aquatic macrophytes across boreal catchments: effects of climate change on aquatic macrophytes. J Biogeogr 38:383–393

Andrake W, Johansen HW (1980) Alizarin red dye as a marker for measuring growth in *Corallina officinalis* L. (Corallinaceae, Rhodophyta). J Phycol 16:620–622

Beck MW, Tomcko CM, Valley RD, Staples DF (2014) Analysis of macrophyte indicator variation as a function of sampling, temporal, and stressor effects. Ecol Indic 46:323–335

Bélanger D, Gagnon P (2020) Low growth resilience of subarctic rhodoliths (*Lithothamnion glaciale*) to coastal eutrophication. Mar Ecol Prog Ser 642:117–132

Bindoff NL, Cheung WWL, Kairo JG, Arístegui J and others (2019) Changing ocean, marine ecosystems, and dependent communities. In: Pörtner HO, Roberts DC, Masson-Delmotte V, Zhai P and others (eds) IPCC special report on the ocean and cryosphere in a changing climate. IPCC, Geneva, p 447–587

Blain C, Gagnon P (2013) Interactions between thermal and wave environments mediate intracellular acidity (H_2SO_4), growth, and mortality in the annual brown seaweed *Desmarestia viridis*. J Exp Mar Biol Ecol 440:176–184

Blake C, Maggs CA (2003) Comparative growth rates and internal banding periodicity of maerl species (Corallinales, Rhodophyta) from northern Europe. Phycologia 42:606–612

Burdett H, Hennige S, Francis F, Kamenos N (2012) The photosynthetic characteristics of red coralline algae, determined using pulse amplitude modulation (PAM) fluorometry. Bot Mar 55:499–509

Caines S, Gagnon P (2012) Population dynamics of the invasive bryozoan *Membranipora membranacea* along a 450-km latitudinal range in the subarctic northwestern Atlantic. Mar Biol 159:1817–1832

Comeau S, Carpenter RC, Edmunds PJ (2014) Effects of irradiance on the response of the coral *Acropora pulchra* and the calcifying alga *Hydrolithon reinboldii* to temperature elevation and ocean acidification. J Exp Mar Biol Ecol 453:28–35

Darrenougue N, De Deckker P, Payri C, Eggins S, Fallon S (2013) Growth and chronology of the rhodolith-forming, coralline red alga *Sporolithon durum*. Mar Ecol Prog Ser 474:105–119

Dring MJ (1990) Light harvesting pigment composition in marine phytoplankton and macroalgae. In: Herring PJ, Campbell AK, Whitfield M, Maddock L (eds) Light and life in the sea. Cambridge University Press, New York, NY, p 59–88

Eggert A (2012) Seaweed responses to temperature. In: Wiencke C, Bischof K (eds) Seaweed biology: novel insights into ecophysiology, ecology and utilization. Ecological Studies 219. Springer-Verlag, Berlin, p 47–66

Epp RW, Lewis WM Jr (1979) Metabolic responses to temperature change in a tropical freshwater copepod (*Mesocyclops brasilianus*) and their adaptive significance. Oecologia 42:123–138

Epp RW, Lewis WM Jr (1980) Metabolic uniformity over the environmental temperature range in *Brachionus plicatilis* (Rotifera). Hydrobiologia 73:145–147

Fabricius KE, De'ath G, Humphrey C, Zagorskis I, Schaffelke B (2013) Intra-annual variation in turbidity in response to terrestrial runoff on near-shore coral reefs of the Great Barrier Reef. Estuar Coast Shelf Sci 116: 57–65

Figueroa FL, Salles S, Aguilera J, Jiménez C and others (1997) Effects of solar radiation on photoinhibition and pigmentation in the red alga *Porphyra leucosticta*. Mar Ecol Prog Ser 151:81–90

Figueroa FL, Martinez B, Israel A, Neori A and others (2009) Acclimation of Red Sea macroalgae to solar radiation: photosynthesis and thallus absorptance. Aquat Biol 7: 159–172

Foster M (2001) Rhodoliths: between rocks and soft places. J Phycol 37:659–667

Freiwald A, Henrich R (1994) Reefal coralline algal buildups within the Arctic Circle: morphology and sedimentary dynamics under extreme environmental seasonality. Sedimentology 41:963–984

Frey DL, Gagnon P (2015) Thermal and hydrodynamic environments mediate individual and aggregative feeding of a functionally important omnivore in reef communities. PLOS ONE 10:e0118583

Gagnon P, Matheson K, Stapleton M (2012) Variation in rhodolith morphology and biogenic potential of newly discovered rhodolith beds in newfoundland and Labrador (Canada). Bot Mar 55:85–99

Gagnon P, Blain C, Vad J (2013) Living within constraints: irreversible chemical build-up and seasonal temperature-mediated die-off in a highly acidic (H_2SO_4) annual seaweed (*Desmarestia viridis*). Mar Biol 160:439–451

Gillooly JF, Brown JH, West GB, Savage VM, Charnov EL (2001) Effects of size and temperature on metabolic rate. Science 293:2248–2251

Hanelt D (1998) Capability of dynamic photoinhibition in arctic macroalgae is related to their depth distribution. Mar Biol 131:361–369

Hickman AE, Moore CM, Sharples J, Lucas MI, Tilstone GH, Krivtsov V, Holligan PM (2012) Primary production and nitrate uptake within the seasonal thermocline of a stratified shelf sea. Mar Ecol Prog Ser 463:39–57

Ichiki S, Mizuta H, Yamamoto H (2000) Effects of irradiance, water temperature and nutrients on the growth of sporelings of the crustose coralline alga *Lithophyllum yessoense* Foslie (Corallinales, Rhodophyceae). Phycol Res 48: 115–120

Kamenos NA, Law A (2010) Temperature controls on coralline algal skeletal growth. J Phycol 46:331–335

Kamenos NA, Cusack M, Moore PG (2008) Coralline algae are global palaeothermometers with bi-weekly resolution. Geochim Cosmochim Acta 72:771–779

Korczynski PC, Logan J, Faust JE (2002) Mapping monthly distribution of daily light integrals across the contiguous United States. Horttechnology 12:12–16

Lang A, Yang S, Kass E (2017) Sea ice thickness and recent Arctic warming. Geophys Res Lett 44:409–418

Levitus S, Antonov JI, Boyer TP, Baranova OK and others (2012) World ocean heat content and thermosteric sea level change (0–2000 m), 1955–2010. Geophys Res Lett 39:L10603

Long MH, Rheuban JE, Berg P, Zieman JC (2012) A comparison and correction of light intensity loggers to photosynthetically active radiation sensors. Limnol Oceanogr Methods 10:416–424

Lüning K (1984) Temperature tolerance and biogeography of seaweeds: the marine algal flora of Helgoland (North Sea) as an example. Helgol Meeresunters 38:305–317

Martin S, Cohu S, Vignot C, Zimmerman G, Gattuso JP (2013) One-year experiment on the physiological response of the Mediterranean crustose coralline alga, *Lithophyllum cabiochae*, to elevated p CO_2 and temperature. Ecol Evol 3:676–693

Millar KR, Gagnon P (2018) Mechanisms of stability of rhodolith beds: sedimentological aspects. Mar Ecol Prog Ser 594:65–83

Ogston AS, Field ME (2010) Predictions of turbidity due to enhanced sediment resuspension resulting from sea-level rise on a fringing coral reef: evidence from Molokai, Hawaii. J Coast Res 26:1027–1037

Quinn GP, Keough MJ (2012) Experimental design and data analysis for biologists. Cambridge University Press, New York, NY

R Core Team (2019) R: a language and environment for statistical computing. R foundation for statistical computing, Vienna

Ragazzola F, Foster LC, Jones CJ, Scott TB, Fietzke J, Kilburn MR, Schmidt DN (2016) Impact of high CO_2 on the geochemistry of the coralline algae *Lithothamnion glaciale*. Sci Rep 6:20572

Riosmena-Rodriguez R, Nelson W, Aguirre J (2017) Rhodolith/maerl beds: a global perspective. Springer, Berlin

Scheibling RE, Gagnon P (2009) Temperature-mediated outbreak dynamics of the invasive bryozoan *Membranipora membranacea* in Nova Scotian kelp beds. Mar Ecol Prog Ser 390:1–13

Schoenrock KM, Bacquet M, Pearce D, Rea BR and others (2018) Influences of salinity on the physiology and distribution of the arctic coralline algae, *Lithothamnion glaciale* (Corallinales, Rhodophyta). J Phycol 54: 690–702

Schwarz AM, Hawes I, Andrew N, Mercer S, Cummings V, Thrush S (2005) Primary production potential of non-geniculate coralline algae at Cape Evans, Ross Sea, Antarctica. Mar Ecol Prog Ser 294:131–140

Snedecor GW, Cochran WG (1994) Statistical methods, 8th edn. Iowa State University Press, Ames, IA

Spilling K, Ylöstalo P, Simis S, Seppälä J (2015) Interaction effects of light, temperature and nutrient limitations (N, P and Si) on growth, stoichiometry and photosynthetic parameters of the cold-water diatom *Chaetoceros wighamii*. PLOS ONE 10:e0126308

Steller DL, Hernádez Ayón JM, Riosmena Rodríguez R, Cabello Pasini A (2007) Effect of temperature on photosynthesis, growth and calcification rates of the free-living coralline alga *Lithophyllum margaritae*. Cienc Mar 33:441–456

Teed L, Bélanger D, Gagnon P, Edinger E (2020) Calcium carbonate ($CaCO_3$) production of a subpolar rhoodlith

bed: methods of estimation, effect of bioturbators, and global comparisons. Estuar Coast Shelf Sci 242:106822

Teichert S, Freiwald A (2014) Polar coralline algal $CaCO_3$ production rates correspond to intensity and duration of the solar radiation. Biogeosciences 11:833–842

Teichert S, Woelkerling W, Rüggeberg A, Wisshak M and others (2012) Rhodolith beds (Corallinales, Rhodophyta) and their physical and biological environment at 80°31′N in Nordkappbukta (Nordaustlandet, Svalbard Archipelago, Norway). Phycologia 51:371–390

Van der Heijden LH, Kamenos NA (2015) Reviews and syntheses: calculating the global contribution of coralline algae to total carbon burial. Biogeosciences 12:6429–6441

White WB, Lean J, Cayan DR, Dettinger MD (1997) Response of global upper ocean temperature to changing solar irradiance. J Geophys Res 102:3255–3266

Wiencke C, tom Dieck I (1990) Temperature requirements for growth and survival of macroalgae from Antarctica and southern Chile. Mar Ecol Prog Ser 59:157–170

Wilson S, Blake C, Berges JA, Maggs CA (2004) Environmental tolerances of free-living coralline algae (maerl): implications for European marine conservation. Biol Conserv 120:279–289

Woelkerling WMJ, Irvine LM, Harvey AS (1993) Growth-forms in non-geniculate coralline red algae (Corallinales, Rhodophyta). Aust Syst Bot 6:277–293

Wozniak B, Dera J (2007) Light absorption in sea water. Atmospheric and Oceanic Sciences Library Vol 33. Springer-Verlag, New York, NY

Zuur AF, Ieno EN, Walker NJ, Saveliev AA, Smith GM (2009) Mixed effects models and extensions in ecology with R. Springer, New York, NY

Editorial responsibility: Morten Pedersen, Roskilde, Denmark
Reviewed by: 3 anonymous referees

Submitted: January 29, 2020
Accepted: January 15, 2021
Proofs received from author(s): March 24, 2021